Synthetic and Systems Biotechnology 9 (2024) 1–10

Contents lists available at ScienceDirect

Synthetic and Systems Biotechnology

journal homepage: www.keaipublishing.com/en/journals/synthetic-and-systems-biotechnology

# EMT transcription factors activated circuits: A novel tool to study EMT dynamics and its therapeutic implications

Tianying Chen [a,1], Wangyue Jia [a,1], Bo Zhang [a], Hanqi Xie [a], Qiong Wu [a,*]

[a] MOE Key Laboratory of Bioinformatics, Center for Synthetic and System Biology, School of Life Sciences, Tsinghua University, Beijing, 100084, China

ARTICLE INFO

*Keywords:*
Epithelial mesenchymal transition
Synthetic biology
Tumor killing

ABSTRACT

The epithelial mesenchymal transition (EMT) plays significant roles in the progression of cancer and fibrotic disease. Moreover, this process is reversible, resulting in mesenchymal epithelial transition (MET), which plays an important role in cancer metastasis. There is a lack of methods to trace and target EMT cells using synthetic biology circuits, which makes it difficult to study the cell fate or develop targeted treatments. In this study, we introduced responsive EMT sensing circuits, which sense the EMT using specific promoters that respond to transcription factors typical of EMT activation (EMT-TFs). The transcriptional strength of EMT-sensing promoters decreased more than 13-fold in response to the overexpression of the EMT-TF. Then, the NOT gate circuits were built by placing the tetR transcription repressor under the control of EMT sensing promoters and expressed an output signal using the constitutive CMV promoter modified with tetO sites This circuit is named EMT sensing and responding circuits .When the EMT transcription factors was present, we observed a 5.8-fold signal increase in the system. Then, we successfully distinguished mesenchymal breast cancer cells from epithelial cancer cells and repressed the proliferation of EMT tumor cells using our circuits. The EMT sensing and responding circuits are promising tools for the identification of EMT cells, which is crucial for EMT-related disease therapy and investigating the mechanisms underlying the reversible EMT process.

## 1. Introduction

The epithelial–mesenchymal transition (EMT) is a process in which cells lose their epithelial characteristics and assume a mesenchymal phenotype. This leads to functional changes in migratory capacity, invasiveness, and changed interactions with the basement membrane, among other significant changes. Under physiological conditions, this genetic program contributes to embryonic development and wound healing, but aberrantly activated EMT is associated with organ fibrosis and tumor progression [1–4]. Moreover, this process is reversible, so that EMT cells can regain epithelial features in a process termed mesenchymal-epithelial transition (MET). During the progression of cancer, there is a shift towards a mobile mesenchymal cell phenotype, which is linked to the capacity to dissociate from the primary tumor, followed by intravasation and escape into circulation. Conversely, it is believed that the MET enables the outgrowth of metastases at the distant site [5,6]. The EMT also occurs at the migrating front of the epidermis during cutaneous wound re-epithelialization, after which keratinocytes eventually resume the epithelial signatures upon the fusion of edges [7]. However, the gene expression profile of EMT cells is not universal and differs significantly under various physiological or pathological conditions. Moreover, cells frequently undergo a partial EMT program without gaining typical mesenchymal traits [4]. Consequently, lineage tracing studies using a single mesenchymal gene such as FSP1, Vimentin, N-cadherin and Tenascin C reached conflicting conclusions about the role played by the reversible epithelial-mesenchymal transition in the progression of cancer [8–11]. These findings indicate that the gene expression profiles of epithelial and mesenchymal states are likely context specific, and thus relying on a small subset of markers may lead to erroneous conclusions about the relative E/M status of cells [12]. The technical challenges facing studies on the tracing of EMT cells make it difficult to unravel the relevance of reversible EMT for cancer metastasis and the formation of scar tissue. Moreover, the mechanism of the mesenchymal-epithelial transition has not been discussed in detail. In addition, the absence of good target genes for influencing EMT cells makes it difficult to treat related diseases using gene therapy

Peer review under responsibility of KeAi Communications Co., Ltd.
* Corresponding author.
*E-mail address:* wuqiong@mail.tsinghua.edu.cn (Q. Wu).
[1] These authors contribute equally to this work.

https://doi.org/10.1016/j.synbio.2023.11.010
Received 8 October 2023; Received in revised form 15 November 2023; Accepted 26 November 2023
Available online 3 December 2023

approaches.

Although there is no universal subset of upregulated mesenchymal genes, the EMT is generally executed by activating transcription factors (EMT-TFs), mainly belonging to the SNAIL, TWIST and ZEB families [13,14]. The hallmark event of the EMT is the downregulation of E-cadherin. There are four EMT-TFs binding sites containing E-box elements in the human E-cadherin gene regulatory sequences (pCDH1), which are bound by EMT-TFs from the SNAIL [15,16], TWIST [17,18] and ZEB [19,20]. These EMT-TFs recruit HDAC and repress transcription.

Since pCDH1 has low transcription intensity, we inserted EMT-TF binding sequences into constitutive mammalian promoters with high transcriptional intensity to develop ubiquitous promoters responsive to the EMT, termed EMT responsive promoters.. In addition, we developed an EMT responsive circuits consisted of a repressor controlled by an EMT responsive promoter combined with the Cre/LoxP system [21] or a suicide gene expressed from the promoter which can be blocked by the repressor. Using this system, the expression of the output is switched on when the EMT occurs (Fig. 1A).

## 2. Material and methods

### 2.1. Mammalian cell culture

Human embryonic kidney cells (HEK293T, ATCC), human breast cancer cells (MCF-7 and MDA-MB-231, ATCC) were cultured in Dulbecco's modification Eagle's medium (DMEM-high glucose, Hyclone), supplemented with an additional 10 % fetal bovine serum (FBS, GIBCO) and 1 % penicillin-streptomycin (PS, Hyclone). All cell cultures were kept under standard culture conditions (5 % CO2 and 37 °C).

### 2.2. Plasmids construction

All plasmids made in this study were generated by standard molecular cloning methods. The inserted DNA fragments were PCR amplified from plasmid using Q5® High-Fidelity 2X (New England Biolabs, NEB), and fragments were constructed using Gibson Assembly® Master Mix (New England Biolabs, NEB). The gibson assembly products were transformed into Trelief® 5α Chemically Competent Master Mix (Tsingke), these cells were cultured in LB medium with 100ug/ml ampicillin or 100ug/ml kanamycin for selection. All plasmids were sequenced for validation by Tsingke Company (Beijing, China), and extracted from cells using QIAprep Spin Miniprep.

pCDH1 sequence was synthesized by Tsingke Company (Beijing, China). EMT sensing promoters constructs was derived from the mEGFP-N1 plasmid (Addgene, #54767), the CMV promoter and CMV enhancer were replaced by EMT sensing promoters. Red fluorescent protein mCherry was expressed by PGK promoter as mark gene.

Snail1, Twist1 and Zeb1coding sequence were synthesized by Tsingke Company (Beijing, China), and expressed by CMV promoter. And blue fluorescent protein BFP was expressed by SV40 promoter as the mark gene.

For the construction of EMT sensing and responding circuits, we clone the TN and TNS plasmids. The red fluorescent protein mCherry was expressed as fluorescent reporter under the CMV-tetO promoter in the TN plasmid. And for TNS, the snail1 protein expressed from CMV promoter was attached to the TN plasmid.

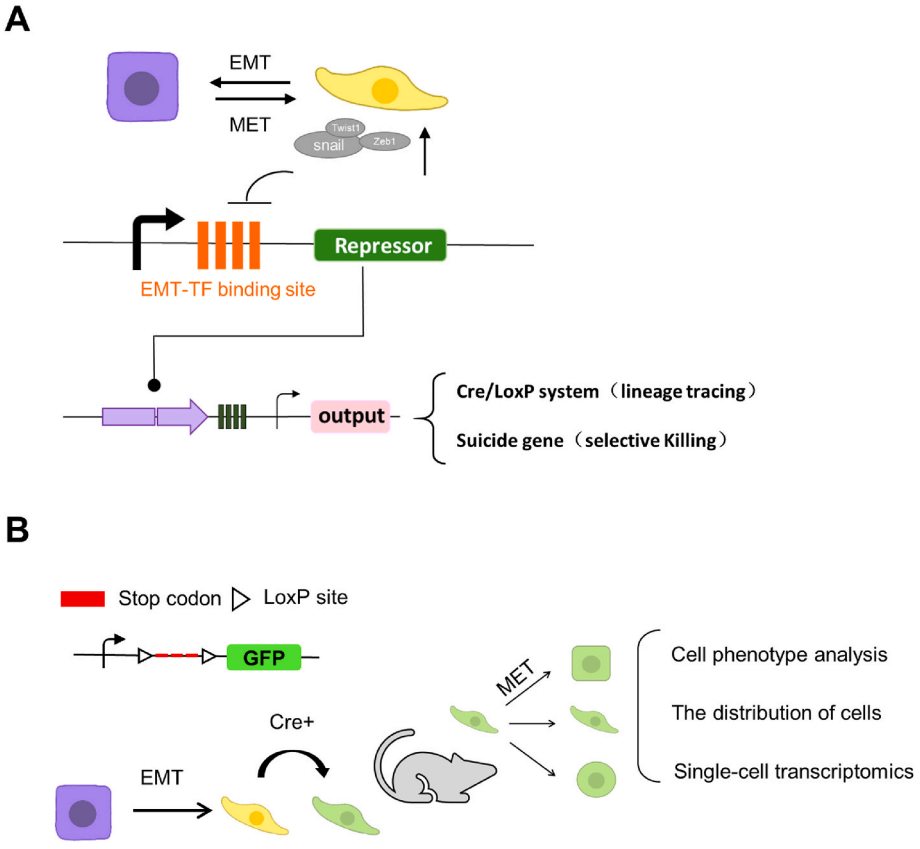


**Fig. 1. EMT sensing and responding circuits were designed to manipulate EMT cells.** (A) EMT sensing promoters were constructed by modifying mammalian constitutive promoters with specific binding sites that are bound by EMT-TFs. In cells in the mesenchymal state, the activity of EMT sensing promoters is inhibited by EMT-TFs. The expression of the transcriptional repressor is therefore downregulated, enabling the activation of the output signal expressed via promoters controlled by the repressor. (B) Cre-recombinase can effectively delete loxP-flanked chromosomal DNA sequences. Cre-recombinases controlled by EMT sensing and responding circuits are expected to be activated in cells in the mesenchymal state, allowing the permanent expression of a fluorescent reporter (such as GFP) downstream of the loxP flanked stop codon cassette. The offspring of labeled EMT cells could be traced and studied, revealing their cell fate and the mechanism of cell fate decisions.

A complete list of plasmids and associated sequences were provided in Supplemental Table 1.

### 2.3. Cell transfections

According to the manufacturer's instructions, all plasmids were transfected into HEK293T cells by Lipo8000 (Beyotime), and into breast cancer cells by Lipofectamine 3000 (Invitrogen). Typically, 2 x 10^5 cells were seeded on a well of 12-well cell culture plates coated. When the confluency of cell was around 50 %, transfection was performed. For Lipofectamine 3000 transfection, we diluted 2ul P3000 reagent into 50ul of OptiMEM (GIBCO), as well as 1.5ul Lipofectamine 3000 and all plasmids into 50ul of OptiMEM per well. For Lipo8000 transfection, we diluted 2ul Lipo8000 reagent and all plasmids into 50ul of OptiMEM per well.

### 2.4. Microscopy images

Seventy-two hours after transfection, plates were removed from the incubator and all wells were examined via AMG EVOS Microscope at room temperature. Cells were imaged using a 10 × objective to photograph fluorescence under brightfield, GFP, and RFP filters, respectively.

### 2.5. RNA isolation and quantitative RT-PCR

Total RNA was extracted from cells using TRIzol reagent (Invitrogen, USA) according to manufacturer's instructions. Then, total RNA (1 μg) was reverse-transcribed using the StarScriptII First-strand cDNA Synthesis Mix with gDNA Remover (GenStar, China). The 2 × RealStar Green Power Mixture with ROXII (GenStar China) was used to label the cDNA with fluorescent probes. Real-time-polymerase chain reaction (RT-PCR) was performed on a 7500 Fast Real-time PCR system (Thermo Fisher Scientific, USA), using the two-step RT-PCR program parameters provided by the manufacturer. The primers are listed in Supplemental Table 2.

Cycle threshold (ΔΔCt) values were calculated by normalization to GAPDH, and the gene expression levels were compared using the 2-ΔΔCt values.

### 2.6. Total protein extraction and Western blot analysis

Total protein was extracted using Lysis Buffer for WB/IP Assays (Yeasen Biotechnology). Protein concentrations were determined using the BCA protein assay (Yeasen, China) according to the manufacturer's instructions. An equivalent amount of protein (20 μg) was subjected to 10 % sodium dodecyl sulfate–polyacrylamide gel electrophoresis (SDS–PAGE) and transferred onto a PVDF membrane (0.45 μm, Merck Millipore, Germany). The membranes were blocked for 30 min with 5 % skimmed milk powder in TBST at room temperature. The blocked membranes were individually incubated overnight at 4 °C with primary antibodies against Fibronectin (1:1000,Abcam, Ab268021), E-cadherin (1:1000, CST, 3195T), Vimentin (1:1000, CST, 5741T),β-actin(1:1000, servicebio,GB5003-100). Then, the membranes were washed and incubated with secondary antibodies (1:5000, CST, USA) for 1 h at 37 °C.The chemiluminescence signal was detected using Enlight buffer (Engreen, China). The optical densities of the bands were quantified using Image Lab software (Bio-Rad, USA) and normalized to GAPDH as internal control.

### 2.7. Flow cytometry and data analysis

Seventy-two hours after transfection, cells were harvested for flow cytometry analysis. To prepare samples into 96-well plates. We aspirated the medium, washed the cells with 100 μL PBS, and added 60 μL of 0.25 % trypsin-EDTA (GIBCO) to digest the cells. Then 120 μL culture medium containing 10 % FBS was added to terminate the digestion and samples were transferred into 96-well plates. Cells were analyzed by LSRFortessa™ flow cytometer (BD Biosciences) running FACSDiva software and the data were processed using the FlowJo (V10).

### 2.8. Lentivirus production and infection

Our lentivirus expression plasmids are derived from pCDH-CMV (Addgene, Plasmid #72265). The HSV/tk expressed by CMV-tetO with or without snail1 overexpression, and the tetR expressed by EMT sensing promoter E10 and E13 were respectively inserted in the lentivrus expression backbone. For CMV-tetO-HSV/tk and CMV-tetO-HSV/tk-snail1 expression construct, the selection marker is fluorescent protein mCherry. And for E10/E13-tetR expression construct, the selection marker is puromycin N-acetyltransferase. The detailed sequences of HSV/tk are shown in Table S1. Then, HEK 293T cells were transfected with the lentivirus expression plasmids, lentivirus packing plasmids PSPAX2 and lentivirus envelope expressing plasmid PMD2. G at a mass ration of 2:3:1. The supernatant containing the lentivirus particles was harvested at 48 h post transfection, filtered through 0.45 μm membrane filter and used to infect 20 % confluent HEK293T, MCF-7 and MDA-MB-231 cells. We screened mCherry-positive cells by flow cytometry to obtain HEK293T, MCF-7 and MDA-MB-231 cells carrying HSV/tk gene. And positive MCF-7 and MDA-MB-231 cells were transfected with E10/E13-tetR lentivirus particles in further. Selection in the presence of puromycin (2 μg/ml, solarbio) was carried out in the regular growth medium for 3 days.

### 2.9. Cell viability assay

HEK293T cells carrying HSV/tk expressed by CMV-tetO promoter with or without snail1 overexpression were transfected with tetR under EMT sensing promoters. Twenty-four hours after transfection, HEK293T cells were seeded in 96-well plate at 5000 cells per well. And 1 μM Ganciclovir (Abcam) was added for induction after 6 h. After twenty-four and 72 h of additional growth, cells were assayed for viability by CCK8 assay (Biodee) according to the manufacturer's protocol. Absorbance was determined at 450 nm. HEK293T cells in the control group were transfected with empty carrier plasmids as controls to calculate cell viability.

### 2.10. Statistical analysis

The reported values served as averages of at least three biological replicates GraphPad and represent two independent biological experiments. GraphPad prism was used for data processing and graphing, and *t*-test was used for p-value testing.

## 3. Results

### 3.1. Construction of EMT sensing promoters

There are four EMT-TF binding sites in the human E-cadherin gene regulatory sequence (pCDH1), one of them behind the transcription start site (Supplementary Fig. 1A). We inserted the four EMT-TF binding sites into the strong mammalian constitutive promoters CMV, hPGK, SV40 and EF1α, resulting in four EMT sensing promoter, named E1, E2, E3 and E4, respectively. We used strong constitutive promoters to ensure the EMT sensing promoters can produce adequate amounts of the transcriptional repressor and thereby reduce the background expression. We next placed the reporter mEGFP under the control of the EMT sensing promoters to test them in human embryonic kidney 293T (HEK293T) cells. We found that the overexpression of EMT-TF snail1 reduced the activity of E1 to the greatest extent, by 2-fold (Supplementary Fig. 1B), while the promoter strength of E1 was more than 5-fold that of pCDH1.

However, there was no clear rationale for the number and position of the EMT-TF binding cites in the EMT sensing promoter. This is important

because increasing the number of EMT-TF binding sites might increase the fold change in response to EMT transcription factors, but it might also impact the expression intensity. Considering these uncertainties, we generate a library of synthetic EMT sensing promoters derived from E1 with different insertion numbers and positions of EMT-TF binding sites. Flow cytometry measurements indicated that the derived EMT sensing promoters E10 and E13 gave higher fold induction (Supplementary Figs. 2A and B). Then, we introduced the β-globin intron with the aim to further increase the promoter strength of EMT sensing promoters. However, the results showed no improvement (Supplementary Fig. 2C). Through iterative optimization of EMT sensing promoters, we obtained E10 and E13. There are 8 EMT-TF binding sites between the CMV promoter sequence and the transcription start site in E10 and E13, while the EMT-TF binding found site downstream from the transcription start site in E10 is absent from E13 (Fig. 2A). Following co-transfection with the two EMT sensing promoters with and without snail1 overexpression plasmids, we observed clear mEGFP fluorescence signals by microscopy in the presence of snail1, and a negligible background in the absence of snail1 (Fig. 2B). Moreover, the promoter activity of E10 and E13 was much stronger than that of the regulatory sequence of E-cadherin pCDH1. Quantification of fluorescence signals by flow cytometry revealed that among mEGFP positive cells, the fold inhibition of E10 and E13 in the presence of snail1 was respectively 13.3- and 12.5-fold, while that of pCDH1 was only approximately 2-fold (Fig. 2C and D). Then, we transfected HEK293T cells with EMT sensing promoters as well as the Twist1 or Zeb1 overexpression plasmids, significant decrease could be observed when EMT-TFs were present, especially in E10 group. But we noticed that the overexpression of Twist1 could result a general down-regulation of fluorescent proteins in HEK293T cells. So we further normalized the fluoresce of EMT sensing promoters with that of CMV groups. The adjusted fold-repression exhibited a 4.2 reduction of E10 with Zeb1, while that with Twist1 was only 1.4 fold (Supplementary Fig. 2D). These results demonstrate that inserting EMT-TF binding sites into strong constitutive promoters is a feasible strategy for constructing EMT sensing promoters with high expression intensity.

### 3.2. Construction of EMT sensing and responding circuits

The aim of this study was to build EMT sensing and responding circuits to identify EMT cells. To achieve this, we adapted a negative-feedback circuit based on the transcription repressor proteins TetR and CI434. The TetR has DNA-binding activity and can bind to the tetO element. The expression of the reporter from the CMV promoter modified with tetO sites (pCMV-tetO) can be repressed by tetR [22]. Similarly, DNA-binding repressor CI434 could recognize the OR434 site and inhibit transcription of CMV promoter modified with the OR434 site (pCMV-OR434) [23]. We placed the expression of tetR and CI434 under the control of EMT sensing promoter E1, while expressing the red fluorescent protein mCherry from the constitutive CMV promoter modified with tetO or434 sites. Compared with CI434, the TetR repressor exhibited lower background activity when it was expressed from the EMT sensing promoter (Supplementary Figs. 3A and B). Therefore, the TetR repressor was used for the development of the EMT sensing and responding circuit.

Next, we tested EMT sensing and responding circuits controlled by E10 and E13 in HEK293T cells (Fig. 3A). At the same time, we mimicked the EMT process by overexpressing the EMT-promoting transcriptional activation factor snail1. Further fluorescence microscopy imaging showed that the presence of snail1 significantly upregulated the expression of mCherry (Fig. 3B). Quantitative fluorescence statistics revealed that TetR expressed using pCDH1 can only reduce the mCherry expression level by approximately 5-fold, while the fold reduction of the EMT sensing and responding circuits controlled by E10 and E13 were approximately 14- and 9-fold, respectively (Fig. 3C). We observed significant activation of EMT sensing and responding circuits controlled by E10 in response to snail1 by flow cytometry analysis (Fig. 3D). To better understand the effect of snail1 overexpression on the fluorescence protein level, we calculated the fold activation normalized to controls, based on the mCherry fluorescence output expressed by pCMV-tetO in the presence and absence of snail1 (NC group). Our data revealed that the EMT sensing and responding circuit based on E10 exhibited a 5.8-fold activation, while that of E13 resulted in 3.7-fold activation (Fig. 3E). In summary, we have successfully designed and implemented EMT sensing and responding circuits. In conjunction with the transcriptional repressor TetR, the EMT sensing and responding circuits based on the engineered promoters E10 and E13 exhibited significant activation in response to EMT-TFs, showcasing their potential for identifying EMT cells.

### 3.3. Detection of EMT in cancer cells

To validate EMT sensing and responding circuits in tumor cells, we took advantage of two well established human breast cancer cell lines, MDA-MB231 which is highly invasive and metastatic, together with MCF-7 which is poorly invasive and non-metastatic [24]. Accordingly, the MCF-7 cells have an epithelial-like morphology while the MDA-MB-231 cells appear elongated and spindle-shaped (Supplementary Fig. 4A). Using quantitative PCR (qPCR) and Western blot analysis, we confirmed that the highly invasive cell line MDA-MB231 expressed the mesenchymal markers Fibronectin and Vimentin, combined with a loss of the expression of cell adhesion molecule E-cadherin(Fig. 4B and C). Moreover, the low expression of two genes encoding desmosome proteins, DSP and JUP, as well as the activation of the EMT transcription factor Zeb1 was demonstrated at transcriptional level in MDA-MB-231 cells (Fig. 4B, Supplementary Fig. 4B). Based on these findings, MCF-7 cells exhibit an epithelial state, while the MDA-MB-231 cells are in a mesenchymal state with the activation of Zeb1.

To test whether EMT sensing and responding circuits could distinguish EMT cancer cells from epithelial cancer cells, we firstly measured the strength of the previously constructed responsive promoters in the two breast cancer cell lines. The results showed that the activity of the CMV promoter was similar in two cell lines, while that of the two EMT responsive promoters E10 and E13 was significantly repressed in MDA-MB-231 by 2.1- and 3.1-fold compared with MCF-7 cells, respectively (Fig. 4D). After this initial validation of the constituent promoters, we introduced the EMT responsive circuits into MCF-7 and MDA-MB-231 cells. We observed a 3.6-fold activation of EMT responsive circuits based on the E13 promoter in MDA-MB-231 cells, normalized to the mCherry fluorescence expressed using pCMV-tetO in MDA-MB-231 or MCF-7 cells (Fig. 4E, Supplementary Fig. 4C). We discovered that this circuit generates a significantly higher signal in cancer cell lines prone to metastasis, as compared to non-metastatic cancer cell lines. Furthermore, we quantitatively analyzed this signal activation by measuring the corresponding fluorescence changes.

### 3.4. Killing of cells undergoing EMT

The EMT program is aberrantly activated in many diseases, and cancer cells undergoing the EMT process often acquire more aggressive phenotypes, such as stemness and drug resistance [25]. Therefore, the identification of these EMT cells would enable a wide range of gene therapy approaches.

HSV-*tk* encodes *a* thymidine kinase, which phosphorylates a prodrug, ganciclovir, to the monophosphate form, leading to cell death [26]. To explore the potential of EMT sensing and responding circuits for killing EMT cells, we delivered a toxic cargo (HSV-*tk* gene) regulated by the EMT sensing and responding circuits into HEK293T cells. According to the design, when EMT-TFs are present, the expression of HSV-*tk* should be activated (Fig. 5A). After transfection, the HEK293T cells were cultured in medium containing 1 μM ganciclovir. To evaluate cell viability, we employed the CCK8 assay [27] and observed that the EMT sensing and responding circuits based on the E13 promoter inhibited cell

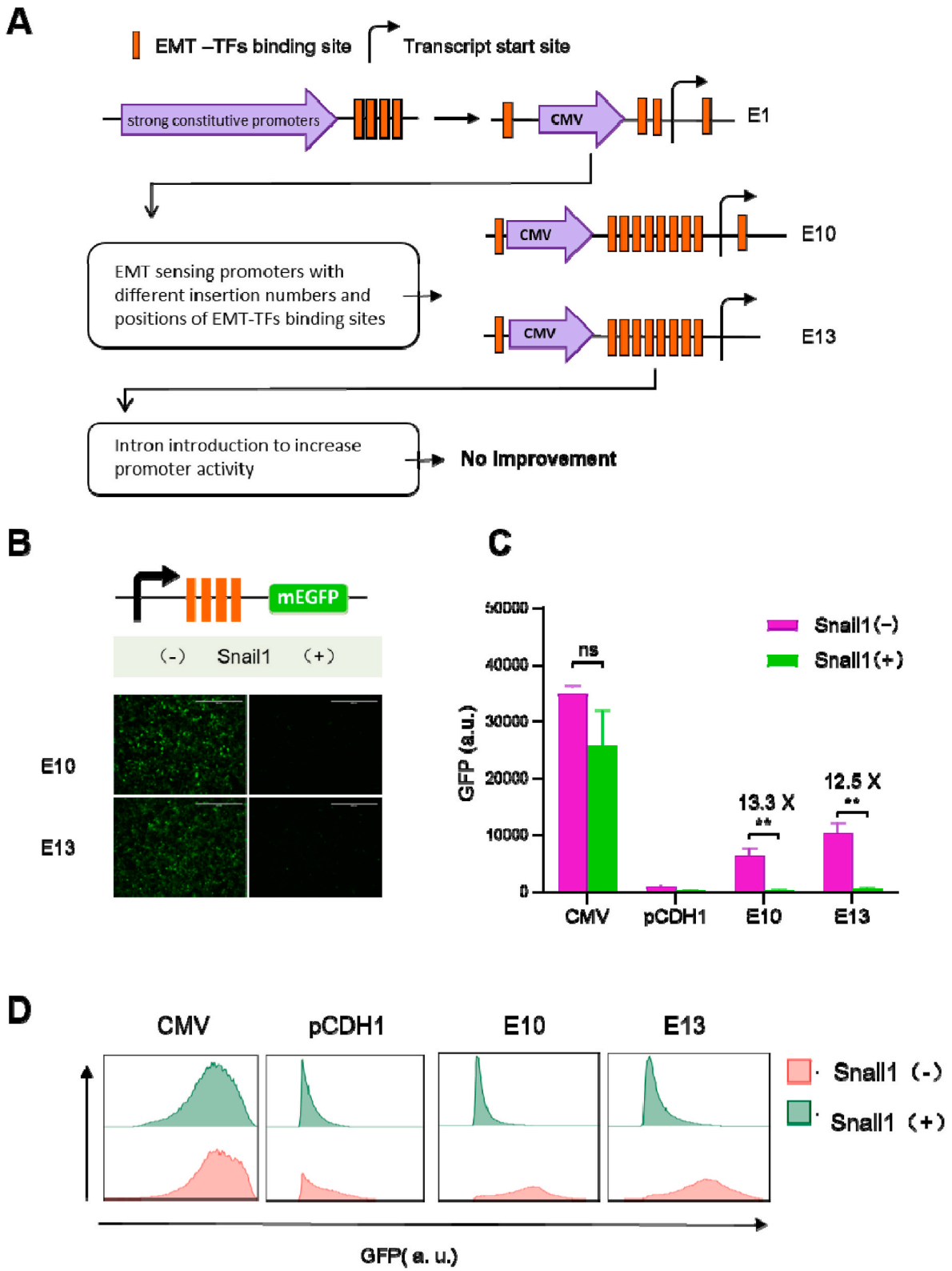


**Fig. 2. Design and characterization of EMT sensing promoters in mammalian cells.** (A) Schematic of the iterative optimization of the EMT sensing promoter. (B) HEK293FT cells were transfected with EMT sensing promoters E10 and E13, controlling the expression of mEGFP, combined with the snail1 overexpression plasmids or control plasmids. Fluorescence micrographs showing HEK293FT cells expressing mEGFP only in the absence of snail1. (C) The fluorescent output of the EMT sensing promoters in HEK293T cell lines with and without snail1. (D) The flow cytometry output distribution of the EMT sensing promoters E10 and E13 in the presence and absence of snail1.

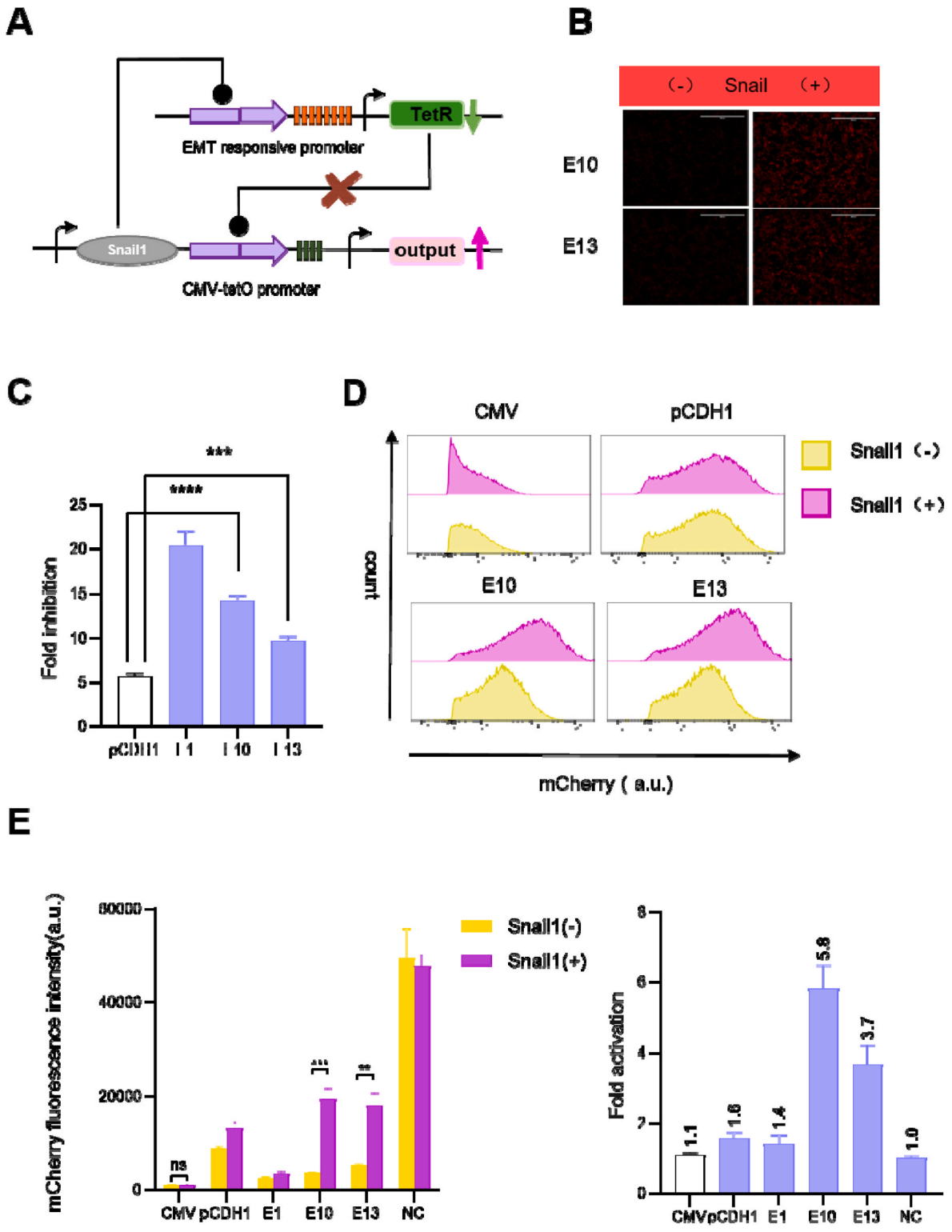


**Fig. 3. Construction of EMT sensing and responding circuits in mammalian cells.** (A) Overview of EMT sensing and responding circuits for detecting EMT cells. When EMT-TFs are absent, the EMT responsive promoters allow the expression of TetR, repressing the pCMV-tetO promoter. As a consequence, the output signal is turned off. Once the epithelial cells transdifferentiate into the mesenchymal state, the EMT responsive promoters are repressed by EMT-TFs (such as snail1). Then, the concentration of TetR in cells decreases, and the output is turned on. (B) HEK293FT cells were transfected with EMT sensing and responding circuits based on the engineered E10 and E13 promoters, with fluorescent mCherry as the signal output, combined with the snail1 overexpression plasmids or control plasmids. Fluorescence micrographs showing HEK293FT cells expressing mCherry only in the presence of snail1.(C) The fold inhibition is calculated as the ratio of the fluorescence output of mCherry expressed from pCMV-tetO (NC group) to that of the EMT responding and sensing circuits in the absence of snial1. (D) The flow cytometry output distribution of the EMT sensing and responding circuits based on E10 and E13 in the presence and absence of snail1. (E) Left, the fluorescence outputs for the EMT sensing and responding circuits in the presence and absence of snail1 in HEK293T cell lines; Right, the fold-activation of EMT sensing and responding circuits. The relative fluorescence was normalized to cells expressing mCherry from the pCMV-tetO promoter (NC group). The fold activation was calculated as the relative fluorescence of EMT sensing and responding circuits in the presence vs. in the absence of snail1.

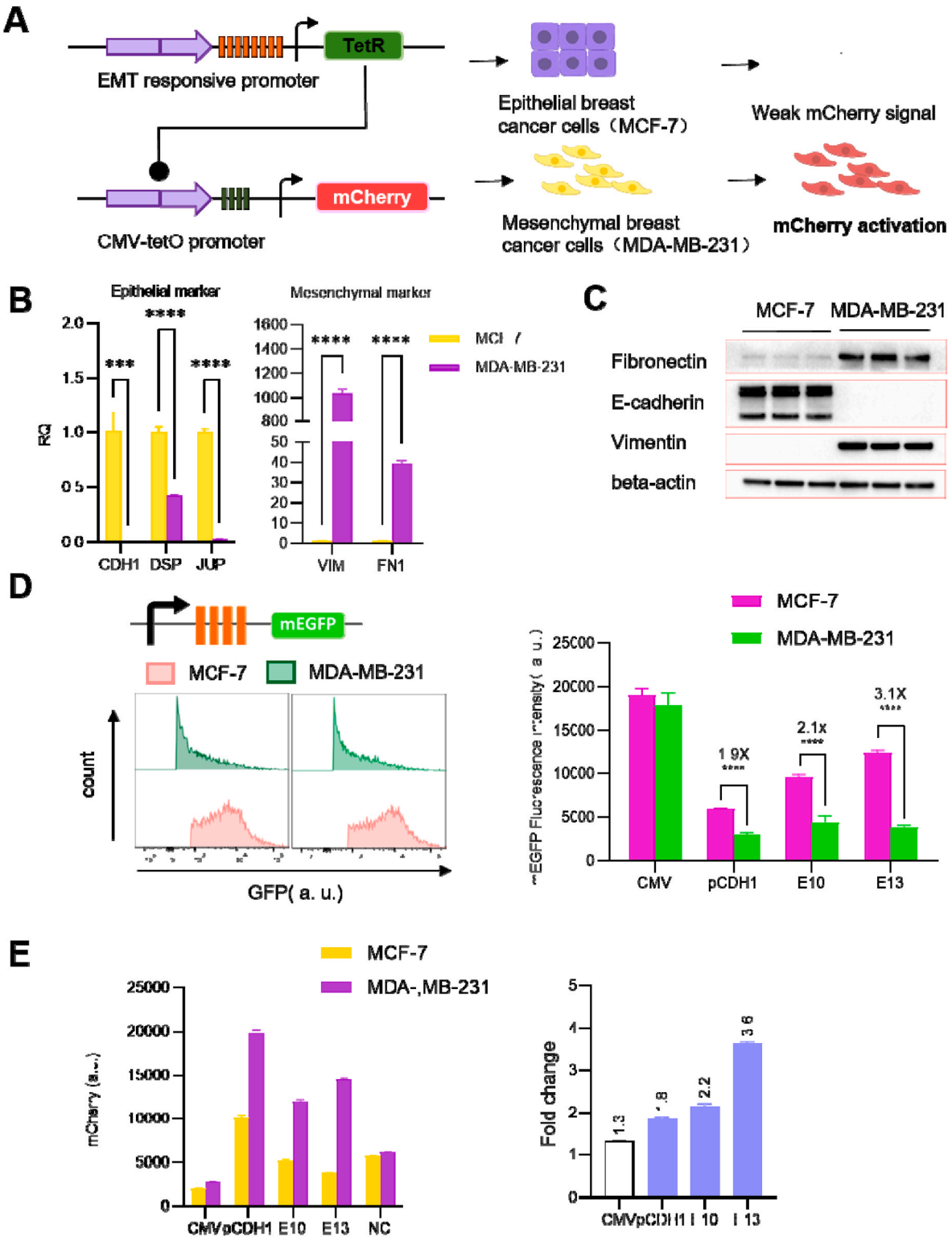


**Fig. 4. Sensing EMT breast cancer cells.** (A) EMT sensing and responding circuits distinguish breast cancer cells in the epithelial state from those in the mesenchymal state.(B) The relative mRNA expression of CDH1 (E-cadherin), DSP, JUP, VIM (vimentin), FN1 (Fibronectin), SNAIL (snail1) and ZEB1 (zeb1) in MCF-7 and MDA-MB-231 cells as assessed by quantitative reverse-transcription PCR (qRT-PCR).(C) Cellular protein levels of fibronectin, vimentin, and E-cadherin in MCF-7 and MDA-MB-231 cells as determined by Western blot analysis with beta-Actin as the internal standard. (D) Left, the flow cytometry output distribution of MCF-7 and MDA-MB-231 cells with circuits based on the EMT sensing promoters E10 and E13; Right, the fluorescent outputs of the EMT sensing and responding circuits in MCF-7 and MDA-MB-231 cells. (E) Left, the fluorescence outputs of the EMT sensing and responding circuits in MCF-7 and MDA-MB-231 cells; Right, The fold activation of EMT sensing and responding circuits; The relative fluorescence was normalized to the expression of mCherry from the pCMV-tetO promoter (NC group) in the MCF-7 cells or MDA-MB-231 cells, respectively; The fold activation was calculated as the relative fluorescence of EMT sensing and responding circuits in the MDA-MB-231 vs. the MCF-7 cells.

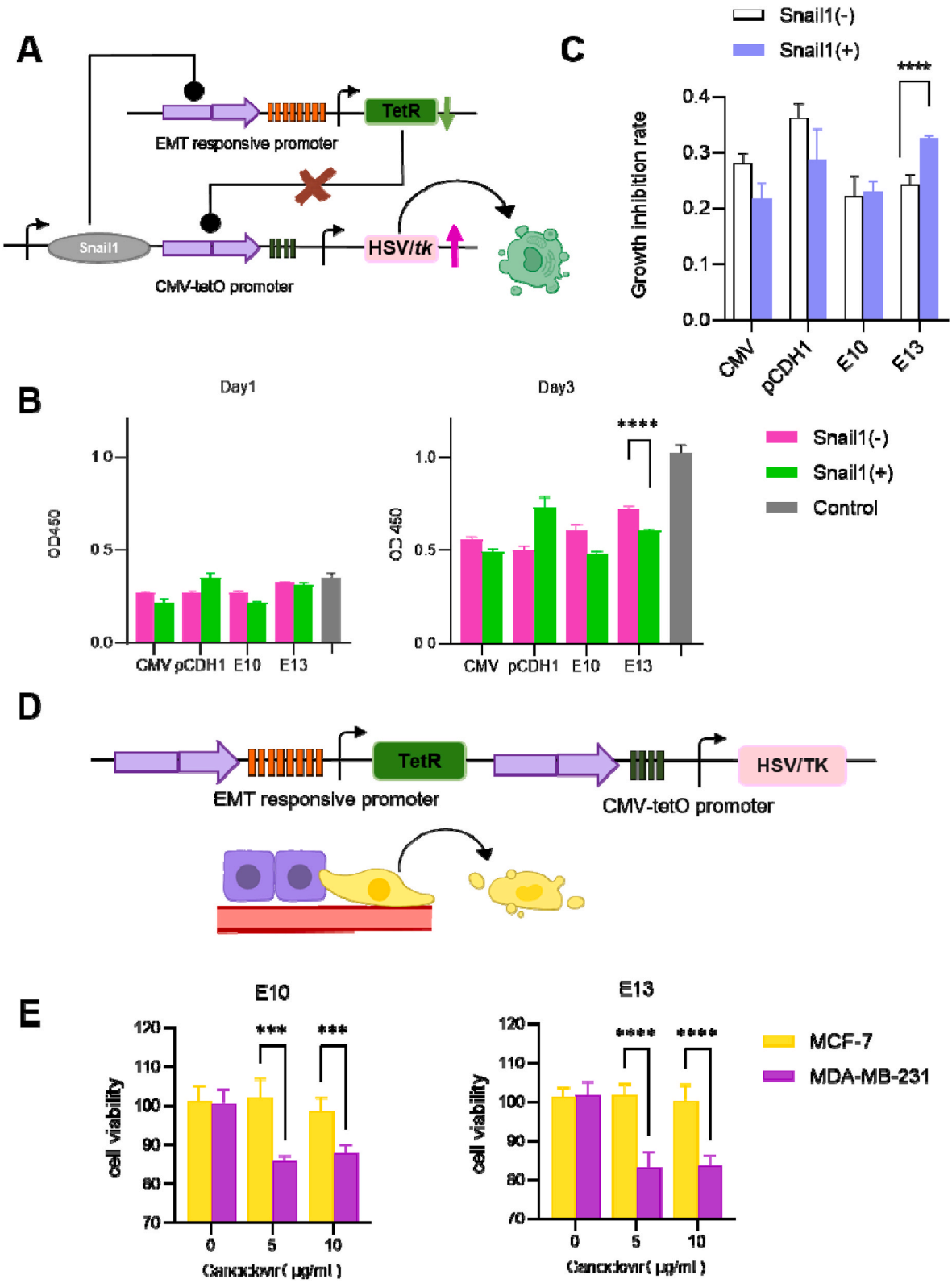


**Fig. 5. Selective killing of EMT cells**. (A) Schematic of EMT sensing and responding circuits that can selectively induce cell death. (B) The growth inhibition rate of HEK293T cells after transfection with the EMT sensing and responding circuits expressing HSV/*tk* in the presence or absence of snail1 after 48h. The relative cell viability was calculated as the ratio of the absorbance at 450 nm between the experimental group and the control group, which was composed of HEK293T cells transfected with a mEGFP expressing plasmid. The growth inhibition rate was defined as the difference between the relative cell viability at 72h to that at 24h. (C) The absorbance at 450 nm of HEK293T cells (CCK8 viability assay), transfected with EMT sensing and responding circuits expressing HSV/*tk* in the presence or absence of snail1 at 24h and 72h. The control group was composed of HEK293T cells transfected with a mEGFP expressing plasmid. (D) EMT sensing and responding circuits selectively kill cancer cells. (E) The viability of MCF-7 and MDA-MB-231 cells after transfection with the EMT sensing and responding circuit expressing the prodrug-converting enzyme gene HSV/tk. To induce cell death, 5 or 10 μg/L GCV was added to the culture medium.

proliferation when snail1 was present(Fig. 5B and C). The relative cell viability was calculated as the ratio of the absorbance at 450 nm between the experimental group and the control group, which consisted of HEK293T cells transfected with a mEGFP expression plasmid. The growth inhibition rate was defined as the difference between the relative cell viability at 24h and that at 72h.

The EMT sensing and responding circuits should ideally selectively kill mesenchymal cancer cells resistant to regular drugs (Fig. 5D). We introduced the EMT sensing and responding circuits into breast cancer cell lines via lentivirus infection. The results revealed that our systems repressed the proliferation of EMT cancer cell line MDA-MB-231 significantly more than that of epithelial cancer cell line MCF-7 when GCV was added to the medium (Fig. 5E). These findings established a basis for effectively targeting EMT cells in clinical therapy using our EMT sensing and responding system.

## 4. Discussion

There is a growing body of evidence suggesting that the activation of the EMT program drives cancer cell stemness and drug resistance, major causes of clinical therapeutic failure [25]. However, the mesenchymal genes that are activated during EMT are widely expressed in non-neoplastic mesenchymal cells such as fibroblasts, which makes it highly challenging to selectively target cancer cells undergoing the EMT with a clinically viable safety margin. In addition, interfering with the TGF-β signaling pathway, which is critical for the activation of EMT, may promote the development of cancer [28,29]. Identification of EMT cancer cells using gene circuits that sense the activation of EMT-TFs provides a new direction for clinical translation. Here, we have developed EMT-sensing promoters and responsive circuits which detect cellular EMT states by sensing the activation of endogenous EMT-TFs. In response to the EMT-TF snail1, the engineered EMT-sensing promoters demonstrated 13-fold downregulation, and the EMT-sensing circuits exhibited 5.8-fold activation. Furthermore, our systems successfully distinguished cancer cells with a mesenchymal phenotype in the activation of Zeb1 from those with an epithelial phenotype, and repressed the proliferation of breast cancer cells undergoing the EMT process. We believe that the EMT responsive circuits hold great potential for applications in EMT cell targeting therapy and tracing.

Although we could detect EMT cells with our system, the fold-induction needs further optimization. Magnifying the signal output requires a more adaptive repressor-based gene expression system, as TetR system cannot be fully repressed with EMT-responsive promoters. However, there are limited bio-bricks and standard parts available at present. Recently, an RNA sensing and responding systems based on ADAR [30,31] and CAS7-11 [32] have been develop, which substantially decrease the cost of targeting EMT cells using different mesenchymal candidate genes. However, the high background activity of these systems limits their application. The combination and integration of various EMT-responsive promoters or circuits may enable more accurate recognition of EMT cells.

By integrating the Cre-loxP system with EMT responding and sensing circuits, we can label EMT cells and track the state of their clonal progeny at a later time point. By analyzing the E/M status and the distribution of the offspring, the cell fate of EMT cells would be revealed. This would allow us to assess the necessity of EMT for cancer cell dissemination and the role played by the reverse process, MET, in the formation of metastases at distant sites. Furthermore, single-cell transcriptomics provides a powerful approach to reconstruct a continuum of cellular E/M states by densely sampling cells at different stages [33]. Based on this, we can infer the gene regulatory network and discovery key factors in the dynamic EMT process from single-cell transcriptional data, offering a promising way to research aspects of the MET that have not been studied in detail to date, laying a foundation for manipulating the reversal of EMT and potentially preventing the spread of metastases (Fig. 1B).

## 5. Conclusion

We constructed EMT sensing and responding circuits based on EMT-TF binding sites found in the promoter of E-cadherin, an epithelial gene universally downregulated or lost in widely studied EMT processes. Our results revealed that the activation of EMT-TFs could decrease the strength of EMT sensing promoters constructed using a strong mammalian constitutive promoter modified with EMT-TF binding sites by more than 10-fold. The EMT sensing promoters could decrease the strength of promoters nearby on the reorganization of Snail1 and Zeb1, while the overexpression of Twsit1 resulted a reduction of the strength of the CMV promoter that we could not validate the responsibility of EMT sensing promoters to Twist1. And by adapting a negative-feedback element, we further constructed EMT sensing and responding circuits, which could distinguish cancer cells in the mesenchymal state with the activation of Zeb1 from those in the epithelial state and selectively inhibit the proliferation of them. This demonstrates the feasibility of identifying EMT cells based on the activation of EMT-TFs. Our circuits are promising tools for identifying and targeting EMT cells more efficiently and comprehensively, providing a new way to eliminate abnormal EMT cells, or label them to study EMT dynamics.

## CRediT authorship contribution statement

**Tianying Chen:** designed the study, wrote the manuscript with input from all authors, performed and analyzed most of the experiments, wrote the manuscript with input from all authors. **Wangyue Jia:** designed the study, performed and analyzed most of the experiments. **Bo Zhang:** performed and analyzed most of the experiments. **Hanqi Xie:** and performed and analyzed most of the experiments. **Qiong Wu:** designed the study, wrote the manuscript with input from all authors.

## Declaration of competing interest

The authors declare the following financial interests/personal relationships which may be considered as potential competing interests:

Wu Qiong reports financial support was provided by the Ministry of Science and Technology of China. Wu Qiong reports financial support was provided by Vanke Special Fund for Public Health and Health Discipline Development, Tsinghua University. Wu Qiong reports financial support was provided by the National Natural Science Foundation of China.

## 6. Acknowledgements

This work was supported by the Ministry of Science and Technology of China (Grant No. 2018YFA0900100), Vanke Special Fund for Public Health and Health Discipline Development, Tsinghua University (NO.20221080049)and the National Natural Science Foundation of China (Grant Nos. 31961133019).

We thank Bin Yu (Core Facility, Center of Biomedical Analysis, Tsinghua University) for technical support with Flow cytometry analysis.

## Appendix A. Supplementary data

Supplementary data to this article can be found online at https://doi.org/10.1016/j.synbio.2023.11.010.

## References

[1] Kalluri R, Weinberg RA. The basics of epithelial-mesenchymal transition. J Clin Investig 2009;119(6):1420–8.
[2] Kalluri R. EMT: when epithelial cells decide to become mesenchymal-like cells. J Clin Investig 2009;119(6):1417–9.
[3] Yang J, et al. Guidelines and definitions for research on epithelial–mesenchymal transition. Nat Rev Mol Cell Biol 2020;21(6):341–52.

[4] Nieto MA, et al. EMT: 2016. Cell 2016;166(1):21–45.
[5] Brabletz S, et al. Dynamic EMT: a multi-tool for tumor progression. EMBO J 2021;40(18):e108647.
[6] Bakir B, et al. EMT, MET, plasticity, and tumor metastasis. Trends Cell Biol 2020;30(10):764–76.
[7] Haensel D, Dai X. Epithelial-to-mesenchymal transition in cutaneous wound healing: where we are and where we are heading. Dev Dynam 2018;247(3):473–80.
[8] Fischer KR, et al. Epithelial-to-mesenchymal transition is not required for lung metastasis but contributes to chemoresistance. Nature 2015;527(7579):472–6.
[9] Bornes L, et al. Fsp1-Mediated lineage tracing fails to detect the majority of disseminating cells undergoing EMT. Cell Rep 2019;29(9):2565–2569.e3.
[10] Li Y, et al. Genetic fate mapping of transient cell fate reveals N-cadherin activity and function in tumor metastasis. Dev Cell 2020;54(5):593–607.e5.
[11] Lüönd F, et al. Distinct contributions of partial and full EMT to breast cancer malignancy. Dev Cell 2021;56(23):3203–3221.e11.
[12] Cook DP, Vanderhyden BC. Context specificity of the EMT transcriptional response. Nat Commun 2020;11(1):2142.
[13] Brabletz T, et al. EMT in cancer. Nat Rev Cancer 2018;18(2):128–34.
[14] Derynck R, Weinberg RA. EMT and cancer: more than meets the eye. Dev Cell 2019;49(3):313–6.
[15] Batlle E, et al. The transcription factor Snail is a repressor of E-cadherin gene expression in epithelial tumour cells. Nat Cell Biol 2000;2(2):84–9.
[16] Liu Y-N, et al. Regulatory mechanisms controlling human E-cadherin gene expression. Oncogene 2005;24(56):8277–90.
[17] Vesuna F, et al. Twist is a transcriptional repressor of E-cadherin gene expression in breast cancer. Biochem Biophys Res Commun 2008;367(2):235–41.
[18] Vesuna F, et al. Twist contributes to hormone resistance in breast cancer by downregulating estrogen receptor-α. Oncogene 2012;31(27):3223–34.
[19] Burk U, et al. A reciprocal repression between ZEB1 and members of the miR-200 family promotes EMT and invasion in cancer cells. EMBO Rep 2008;9(6):582–9.
[20] Meidhof S, et al. ZEB 1-associated drug resistance in cancer cells is reversed by the class I HDAC inhibitor mocetinostat. EMBO Mol Med 2015;7(6):831–47.
[21] Ray MK, Fagan SP, Brunicardi FC. The Cre–loxP system: a versatile tool for targeting genes in a cell-and stage-specific manner. Cell Transplant 2000;9(6):805–15.
[22] Nevozhay D, Zal T, Balázsi G. Transferring a synthetic gene circuit from yeast to mammalian cells. Nat Commun 2013;4(1):1451.
[23] Lou C, et al. Synthesizing a novel genetic sequential logic circuit: a push-on push-off switch. Mol Syst Biol 2010;6(1):350.
[24] Sharma MR, et al. Angiogenesis-associated protein annexin II in breast cancer: Selective expression in invasive breast cancer and contribution to tumor invasion and progression. Exp Mol Pathol 2006;81(2):146–56.
[25] Shibue T, Weinberg RA. EMT, CSCs, and drug resistance: the mechanistic link and clinical implications. Nat Rev Clin Oncol 2017;14(10):611–29.
[26] Oishi T, et al. Efficacy of HSV-TK/GCV system suicide gene therapy using SHED expressing modified HSV-TK against lung cancer brain metastases. Molecular Therapy-Methods & Clinical Development 2022;26:253–65.
[27] Fan Y, et al. CircNR3C2 promotes HRD1-mediated tumor-suppressive effect via sponging miR-513a-3p in triple-negative breast cancer. Mol Cancer 2021;20(1):1–22.
[28] Bierie B, Moses HL. TGFβ: the molecular Jekyll and Hyde of cancer. Nat Rev Cancer 2006;6(7):506–20.
[29] Massagué J. TGFβ signalling in context. Nat Rev Mol Cell Biol 2012;13(10):616–30.
[30] Jiang K, et al. Programmable eukaryotic protein synthesis with RNA sensors by harnessing ADAR. Nat Biotechnol 2023;41(5):698–707.
[31] Kaseniit KE, et al. Modular, programmable RNA sensing using ADAR editing in living cells. Nat Biotechnol 2023;41(4):482–7.
[32] Strecker J, et al. RNA-activated protein cleavage with a CRISPR-associated endopeptidase. Science 2022;378(6622):874–81.
[33] Wagner DE, Klein AM. Lineage tracing meets single-cell omics: opportunities and challenges. Nat Rev Genet 2020;21(7):410–27.